

Ballistic Impact Simulations of an Aluminum 2024 Panel Using *MAT_224 in LS-DYNA[®] Considering Oblique Incidence and Attitude Angles of a Rectangular Projectile

C. K. Park¹, G. Queitzsch (retired)², K. Carney¹, P. Du Bois¹, C. D. Kan¹, D. Cordasco³,
and W. Emmerling³

¹George Mason University, Center for Collision Safety and Analysis, Fairfax, VA

²Federal Aviation Administration, Washington, DC

³Federal Aviation Administration, William J. Hughes Technical Center, NJ

Abstract

*The objective of this study is (1) to validate the *MAT_224 model for Aluminum 2024 with complex impact conditions, (2) to evaluate its predictability of ballistic limit and residual velocities of a projectile under various impact conditions, and (3) to investigate the effects of oblique and attitude angle variations of a projectile on penetration to a target plate. The newly developed *MAT_224 model (version 2.0) for Aluminum 2024 was utilized to simulate a series of ballistic impact tests conducted by NASA using a rectangular block projectile of Inconel 718 with sharp edges and corners, impacting Aluminum 2024 flat panels at oblique angles of incidence. A full ballistic impact simulation model was created with over twenty million solid elements and used to conduct approximately one hundred ballistic impact simulations. Overall, the ballistic impact simulations showed highly comparable results with the NASA tests in terms of projectile residual velocities, failure shapes of the target plates, and projectile penetration behavior. Based on a series of ballistic impact simulations, the ballistic limit velocities of the projectile were predicted.*

Introduction

A team consisting of George Mason University (GMU), Ohio State University (OSU), George Washington University (GWU), the National Aeronautics and Space Administration (NASA) - Glenn Research Center (GRC), and the Federal Aviation Administration (FAA) - Aircraft Catastrophic Failure Prevention Research Program (ACFPP) has collaborated to develop a new material model in LS-DYNA for metallic materials. The research was directed towards improving the numerical modeling of turbine engine blade-out containment tests required for certification of aircraft engines [Emmerling 2014]. The LS-DYNA constitutive material model *MAT_TABULATED_JOHNSON_COOK, or simply *MAT_224, was developed [Buyuk 2014, LSTC 2017]. *MAT_224 is a general elasto-visco-plastic material model incorporating arbitrary stress versus strain curves to define material plasticity, including arbitrary strain rate and temperature dependency. The element erosion criterion is the plastic failure strain, which can be defined as a function of the state of stress, strain rate, temperature and element size.

The original *MAT_224 input parameters (version 1.3) for Aluminum 2024-T351 alloy were developed [Buyuk 2014] based on tabulated data from several material tests performed by OSU [Seidt 2014]. However, the original model did not produce simulations that accurately matched the ballistic impact tests. In addition, continuing research to develop material models for Titanium 6Al-4V and Inconel 718 alloys revealed deficiencies in the original Aluminum mechanical test data. Improved measurement techniques in material tests have since been developed, along with new test methods that provide additional model calibration points on the failure surface. Based on this later work, the updated *MAT_224 input parameters (version 2.0) for Aluminum 2024-T351 alloy were developed and released recently [Park 2020].

NASA conducted a series of ballistic impact tests to provide experimental data to evaluate the numerical material model under more extreme conditions, using a rectangular parallelepiped shaped projectile with sharp corners and edges (45° chamfer to minimize handling damage and reduce numerical sensitivity), impacting flat panels at oblique angles of incidence [Ruggeri 2015]. In the tests, a rectangular block of Inconel 718 impacts an Aluminum 2024 flat panel with various impact velocities (140 fps (feet per second) ~ 350 fps), impact locations (center and off-center), oblique impact angles (0°, 30°, and 45°), and projectile roll angles (0°, 30°, 60°, and 90°). Based on the combination of various impact conditions, 11 test setups were considered and 34 impact tests were conducted.

The objective of this study is (1) to validate the new material model with complex impact conditions, (2) to evaluate the predictability of ballistic limit velocities of a projectile under various impact conditions, and (3) to investigate the effects of oblique and attitude angle variations of the rectangular projectile on penetration of the target plate. The newly developed *MAT_224 for Aluminum 2024 was utilized to conduct a series of ballistic impact simulations of the NASA tests. As a result, over 100 ballistic impact simulations were conducted and their results were analyzed.

NASA Ballistic Impact Tests

The hollow rectangular parallelepiped shaped projectile with sharp corners and edges that was designed for the NASA ballistic tests is shown in Figure 1(a). The nominal dimensions of the projectile are 55.88 mm long, by 31.75 mm high, and by 20.83 mm wide. The projectile was manufactured from Inconel 718 and heat treated to a hardness of 44 Rockwell C. Three rectangular channels were machined through the center of the projectile in the long direction to reduce the overall mass and effective density. The mass of the projectiles ranged from 220.45 to 222.45 gm with an average of 221.52 gm.

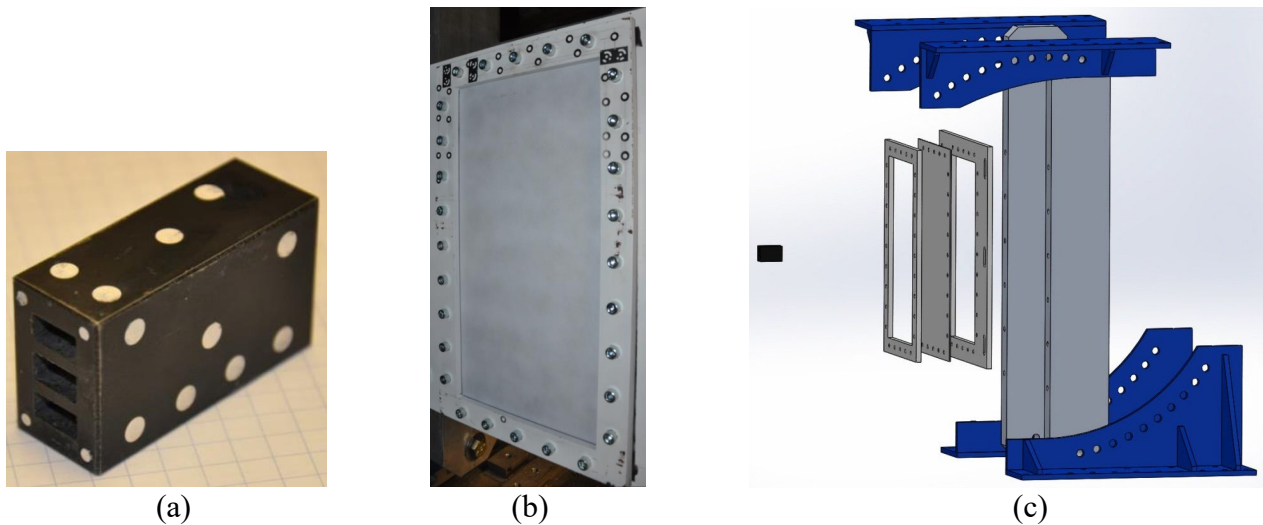


Figure 1. Description of test setup [Ruggeri 2015]: (a) projectile, (b) panel, (c) exploded view of setup.

The typical rectangular impact test panel is shown in Figure 1(b). The nominal dimensions of the panel are 30.48 cm wide, by 53.34 cm long, and 3.20 mm thick. The panel material is Aluminum 2024-T3. The panels were sandwiched between 12.7 mm thick front and back frames with an aperture of 22.86 cm wide by 45.72 cm tall. The front frame has outer dimensions the same as the test panel. The panels were attached by twenty-eight through bolts connecting the front frame, panel and back frame. The frames were fixed to the two columns and the columns were fixed to the top and bottom fixtures as shown in Figure 1(c). The columns were rotated to tilt the panel angle.

In the ballistic impact tests, the rectangular projectile impacts the Aluminum 2024 flat panel under various impact conditions (projectile velocity and orientation) and four impact settings (location on the target and target orientation).

- (1) The two impact locations are at the center and at the off-center quarter point of the panel. The off-center impact point is located at 3/4 of the distance from the bottom of the test panel to the top along the centerline of the panel width for all the off-center impact location cases.
- (2) The three target panel tilt angles are 0°, 30°, and 45°.
- (3) The four projectile roll angles are 0°, 30°, 60°, and 90°.
- (4) The impact velocity of projectile was varied from 140 fps to 350 fps to identify the ballistic limit velocity.

Based on the combination of different impact settings, 11 test setup cases were considered and 34 impact tests were conducted. One test setup is shown in Figure 1(c). In this NASA test series, the oblique angle (α) is defined by the panel tilt angle, and the attitude angle was determined by the roll angle of the projectile. Basically, there are three impact configurations, such as face, edge and corner impacts, based on the initial contact geometry of the projectile to the flat plate. Controlling the test setup with these two variables provided all of the desired face, edge, and corner impact conditions. During the impact tests, the exit velocities of the projectile were measured. The details for the NASA ballistic impact tests are described in the reference by Ruggeri (2005).

Ballistic Impact Finite Element Model

Finite Element (FE) models of the Inconel projectile and the Aluminum plate were developed in LS-DYNA. These models were created using all solid elements. The fixture supporting the target plate was not modeled because the size of the projectile is much smaller than the impact surface of the plate and the impact location on the plate is far enough away from the plate boundary to make fixture boundary effects inconsequential relative to the ballistic impact simulations. In addition, not modeling the fixture hardware helps reduce the number of elements in the overall system model. For all simulations, the plate edge boundaries were all fixed. All of the ballistic impact simulation models were created with the 0.26 mm element size (12 elements through the plate thickness) and reduced element integration scheme.

The *MAT_224 input parameters (version 2.0) for Aluminum 2024-T351 alloy, which were developed and released recently [Park 2020], was used for the plate. The updated material model was validated by a series of ballistic impact tests using spherical and cylindrical projectiles normal to Aluminum 2024 panels of various thicknesses [Park 2020]. Overall, the ballistic impact simulations using the updated material model show a relatively good match to the tests. Table 1 shows the *MAT_224 input parameters for the Aluminum 2024 alloy. The tables and curves for *MAT_224 Aluminum 2024 are shown in Figure 2. The details for the material model development are described in the reference by Park (2020).

Table 1. *MAT 224 Input Parameters of Aluminum 2024.

Column	1	2	3	4	5	6	7
Card1	MID	RO	E	PR	CP	TR	BETA
Input (unit)	-	2.6E-9 (ton/mm ³)	70,000.0 (MPa)	0.3	9.0E+8 (kJoules/ton-Kelvin)	300.0 (Kelvin)	0.4
Card2	LCK1	LCT	LCF	LCG	LCH	LCI	
Input	Table	Table	Table	Curve	Curve	Table	

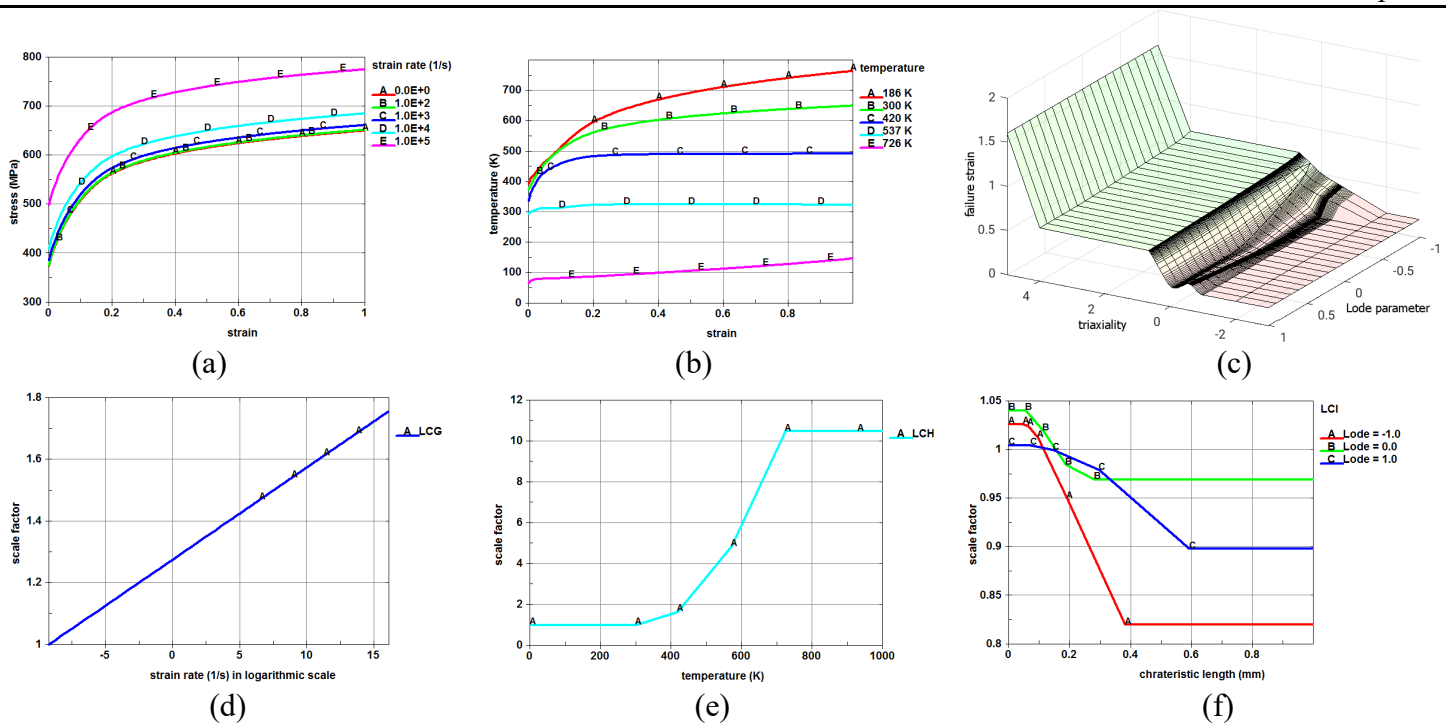


Figure 2. Tables and curves of *MAT_224 of Aluminum 2024: (a) LCK1, (b) LCKT, (c) LCF, (d) LCG, (e) LCH, and (f) LCI.

An Inconel 718 *MAT_224 material model [Dolci 2016], which has a complete plasticity definition and failure model undefined, was used for the projectile. This is acceptable because the deformation of the projectiles was minimal in the ballistic impact tests.

Ballistic Impact Simulations

The ballistic impact simulations of the eleven test setups were conducted with various impact velocities to identify the ballistic limit and residual velocities of the projectile in those test conditions. The ballistic limit velocity is the velocity at which the projectile will penetrate the target panel with zero residual velocity. To find the ballistic limit for a given test setup, the impact velocity of the projectile was varied from 150 fps to 400 fps at 50 fps intervals. In order to reduce simulation runtime, an appropriate symmetric model was used if the symmetry condition was applicable. The quarter symmetry, half symmetry and full models contain approximately 5 million, 10 million and 20 million solid elements respectively.

The impact configurations of the 11 test setups can be classified as face, edge and corner impact cases, based on the initial contact geometry of the projectile to the plate. In the face impact cases, the front face of the rectangular projectile contacts the surface of the plate. In the edge impact cases, the short and mid edges of the rectangular projectile contact the surface of the plate. In the corner impact cases, the corners of the rectangular projectile contact the surface of the plate. The simulations used the nominal attitude and oblique angles in the original test setups. It should be noted that measured angles at impact in the experiment deviated from the desired nominal values.

Figure 3 shows the exit velocities of the projectile over the initial impact velocities used in the tests (blue squares) and simulations (red triangles). The reference line (red dot line) bounds the results with a no velocity change ceiling. The fitting lines through the data points of exit velocities in simulations were determined based on a generalization of an analytical model originally proposed by Recht (1963). The equation of residual velocities is expressed as

$$v_r = a(v_i^p - v_{bi}^p)^{1/p}, \quad (1)$$

where v_r is the residual (or exit) velocity, v_i is the initial velocity, v_{bi} is the ballistic limit velocity, and a and p are the empirical constants [Børvik 2010]. The fit curve (green line) over the exit velocities of the projectile in simulations was approximated by finding the combination of parameters (ballistic limit velocity and two empirical constants) in Equation (1) to make a Root Mean Square (RMS) error minimum.

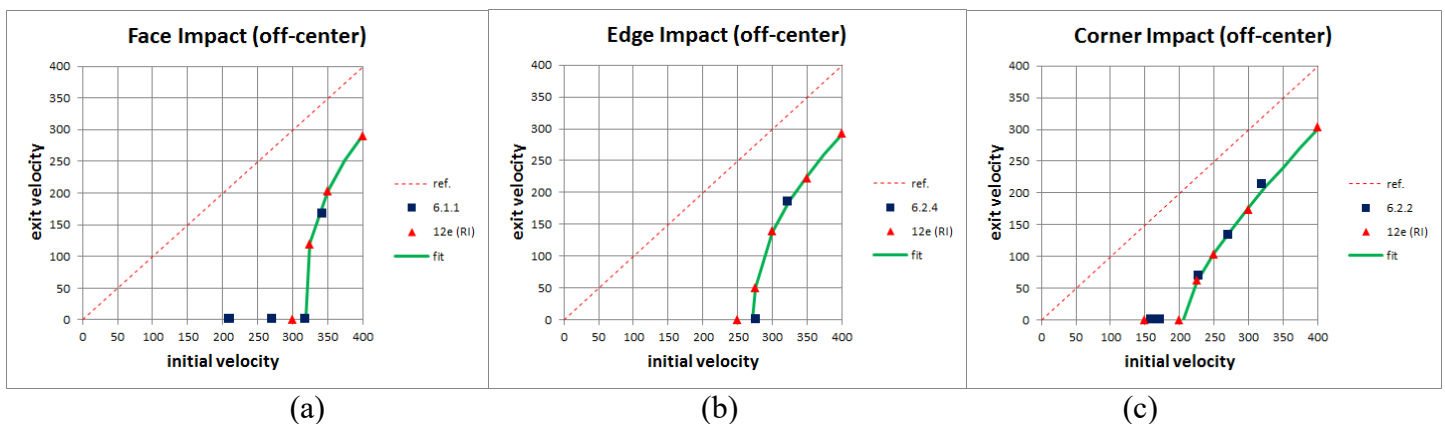


Figure 3. Exit velocities of the projectile (unit: fps): (a) face impact case (#6.1.1), (b) edge impact case (#6.2.4) and (c) corner impact case (#6.2.2).

In most cases, the simulation data points correlate very closely with the test points. In some cases, the exit velocities in the simulations are lower than those in the tests. This could be caused by the mismatch of the mesh patterns between the contact surfaces of the projectile and the target plate and will require further study. In addition, the large angle variation of the projectile in the test could also have caused the discrepancy in the projectile exit velocity between tests and simulations.

The noticeable difference between tests and simulations in the face impact cases is the penetration shapes observed in the target plates. Figure 4 shows the penetration shapes in the face impact case. The size of the penetration hole in the tests is larger than that in the simulations. There is always a 2° to 3° attitude angle variation in the face impact tests. In the face impact case, the attitude angle variation is very sensitive to not only the projectile exit velocity but also the penetration shape of the plate. Figures 5 and 6 show the penetration shapes of the edge and corner impact cases. In both edge and corner impact cases, the penetration shapes between the tests and simulations are quite similar.

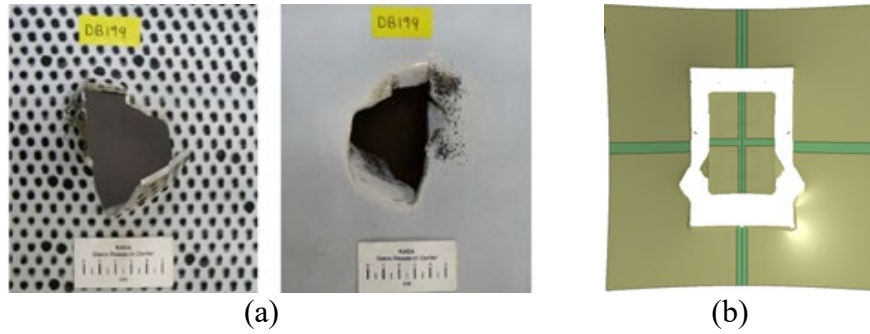


Figure 4. Penetration shape in face impact case (#6.1.1): (a) test (DB199, impact velocity = 343 fps) [Ruggeri 2015] and (b) simulation (impact velocity = 350 fps).

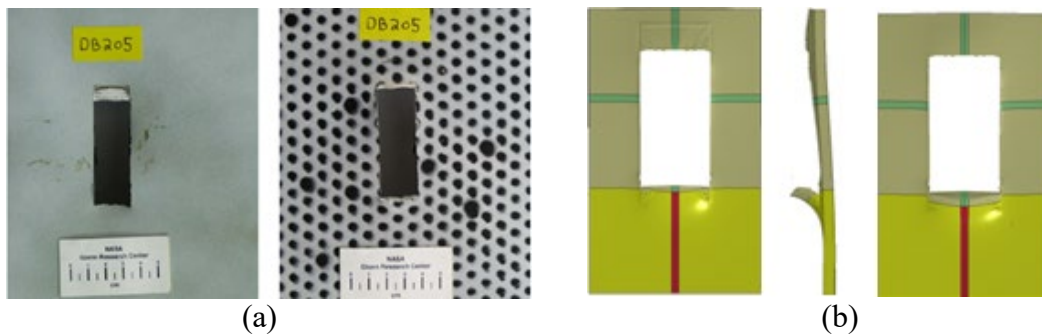


Figure 5. Penetration shape in edge impact case (#6.2.1): (a) test (DB205, impact velocity = 275 fps) [Ruggeri 2015] and (b) simulation (impact velocity = 250 fps).

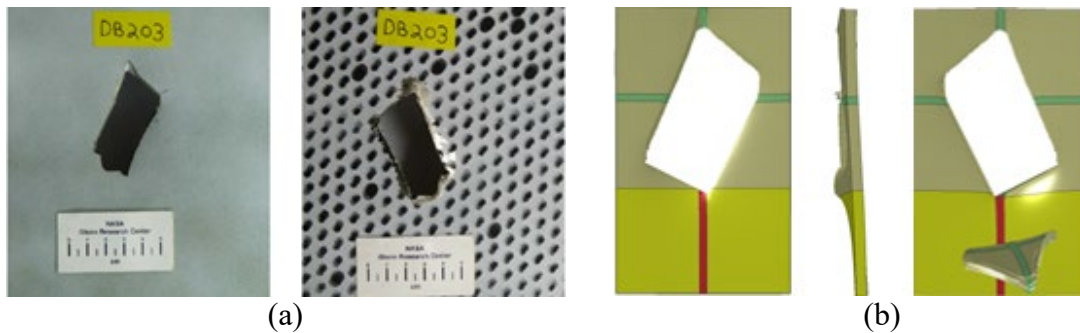


Figure 6. Penetration shape in corner impact case (#6.2.2): (a) test (DB203, impact velocity = 228 fps) [Ruggeri 2015] and (b) simulation (impact velocity = 250 fps).

Sensitivity Analysis of Oblique and Attitude Angles in Ballistic Impact

The sensitivity of oblique and attitude angles of a rectangular projectile in ballistic impact was studied by conducting ballistic impact simulations with varying oblique and attitude angles.

Oblique Angle Variation

In order to find how the oblique angle affects the exit velocity of the projectile, two series of ballistic impact simulations are conducted. Starting from the baseline (#6.1.1) which is the face impact, the projectile tilt angle is changed from 0° to 45° with a 5° interval, which becomes the edge impact series. In another series, the projectile roll angle is set to 30° and then the projectile tilt angle is changed from 0° to 45° with a 5° interval, which becomes the corner impact series. The impact velocity of the projectile in all simulations of the oblique angle variation series was set to 400 fps.

Figure 7 shows the exit velocities of the projectile in two oblique angle variation simulation series. It is confirmed that the exit velocity of the projectile varies as the oblique angle varies and both oblique angle variation series show a very similar trend. The variation ranges of the exit velocities are 56 fps in the edge impact cases and 69 fps in the corner impact cases. The exit velocity of the projectile becomes the lowest as the oblique angle is 5° and the exit velocity becomes the highest as the oblique angle is 25°. The highest exit velocities of the projectile in two oblique angle variation series are similar, but the lowest exit velocities in the edge impact cases of the oblique angle variation series is about 20 fps higher than that in the corner impact cases of the oblique angle variation series.

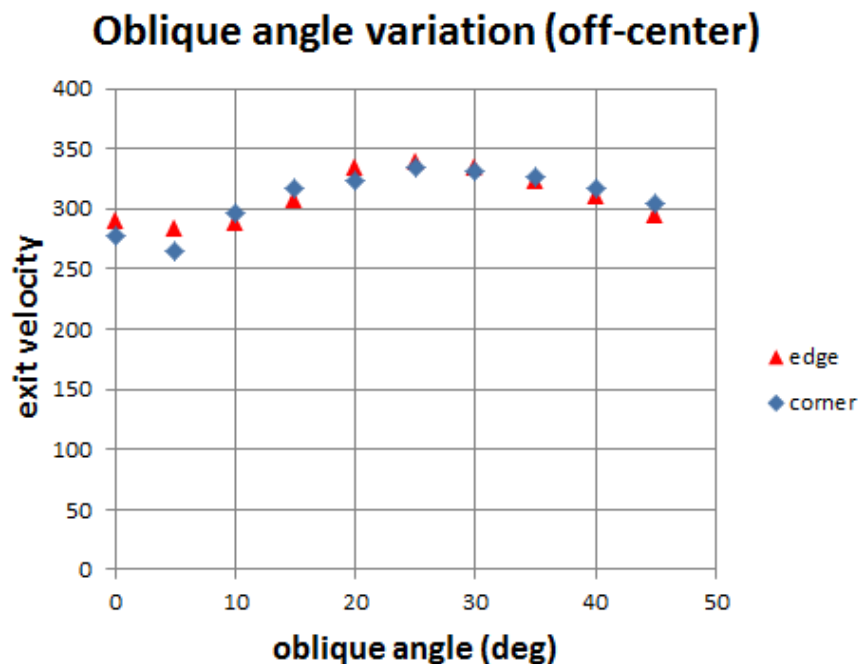


Figure 7. Plot of the exit velocities of the projectile in two oblique angle variation series

Attitude Angle Variation

In the tests, the projectile was set in a certain posture by changing the roll angle and shot to the plate. However, the measured roll, pitch and yaw angles of the projectile varied as high as 15° in the tests. In order to find how the attitude angle affects the exit velocity of the projectile, four series of ballistic impact simulations are conducted. Starting from the baseline (#6.1.1) that is the face impact, four attitude angle variation series were considered:

- Roll angle variation: (1,0,0), (2,0,0) and (3,0,0),
- Pitch angle variation: (0,-3,0), (0,-2,0), (0,-1,0), (0,1,0), (0,2,0) and (0,3,0),
- Yaw angle variation: (0,0,1), (0,0,2) and (0,0,3), and
- Pitch and yaw angle variation: (0,-3,3), (0,-2,2), (0,-1,1), (0,1,1), (0,2,2) and (0,3,3),

where the parenthesis means (roll angle, pitch angle, yaw angle) in degree. In all ballistic simulations of the attitude angle variation series, the oblique angle was set to 0°. The results of the ballistic impact simulations show that the exit velocity of the projectile is sensitive to the oblique angle when the impact velocity is high enough to the ballistic limit velocity. On the other hand, the ballistic limit velocity is more sensitive to the attitude angle of the projectile than the oblique angle. The estimated ballistic limit velocity of the baseline (#6.1.1) in the simulation is 318 fps. So, the impact velocity of the projectile in all ballistic simulations of the attitude angle variation series was set to 325 fps to see the attitude angle variation effects to the ballistic limit velocity as well.

Figure 8 summarizes the exit velocities of the projectile in all the simulations of the attitude angle variation series. Based on the baseline, which is in black, the red means the case that the exit velocity of the projectile decreases and the blue means the case that the exit velocity increases. It can be confirmed that there is a large variation in the exit velocity as the attitude angle varies. The variation range based on the baseline is 86 fps from 75 fps (-37%) to 161 fps (34%). The exit velocity is increased in the pitch angle variation, but it is decreased in other variations mostly.

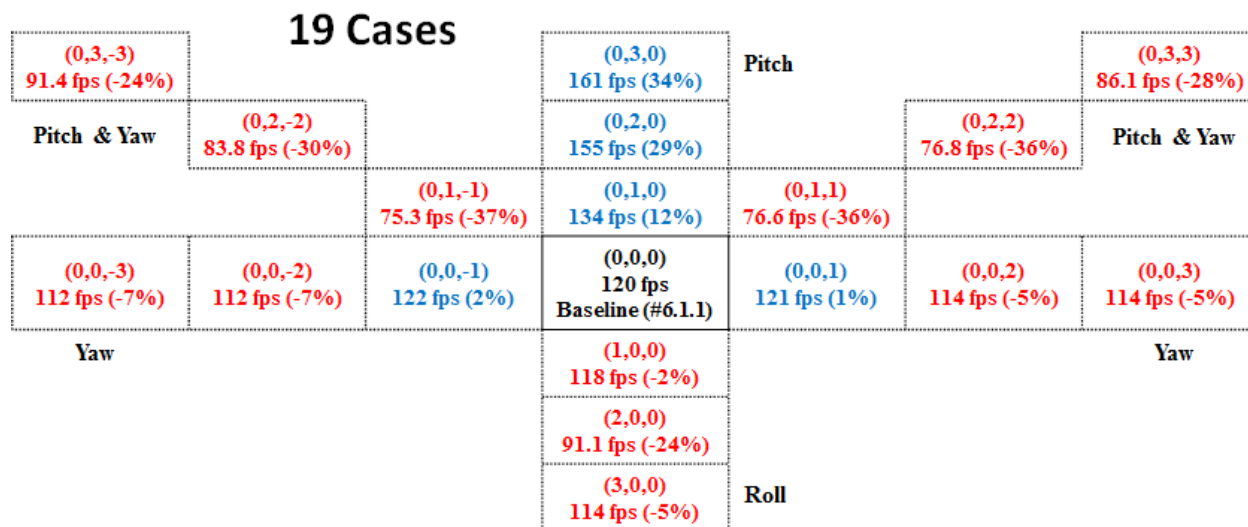


Figure 8. Exit velocities of the projectile in attitude angle variation series (red or blue indicate the decrease or increase of the exit velocity than the baseline respectively)

Figure 9 shows the penetration shapes of the plate in all the simulations of the attitude angle variation series. It can be observed that the penetration shapes are different from the baseline as the attitude angle varies. Noticeably, the penetration holes are much larger in the cases with both pitch and yaw angle variations than others, which causes a large decrease of the exit velocity as shown in Figure 8.

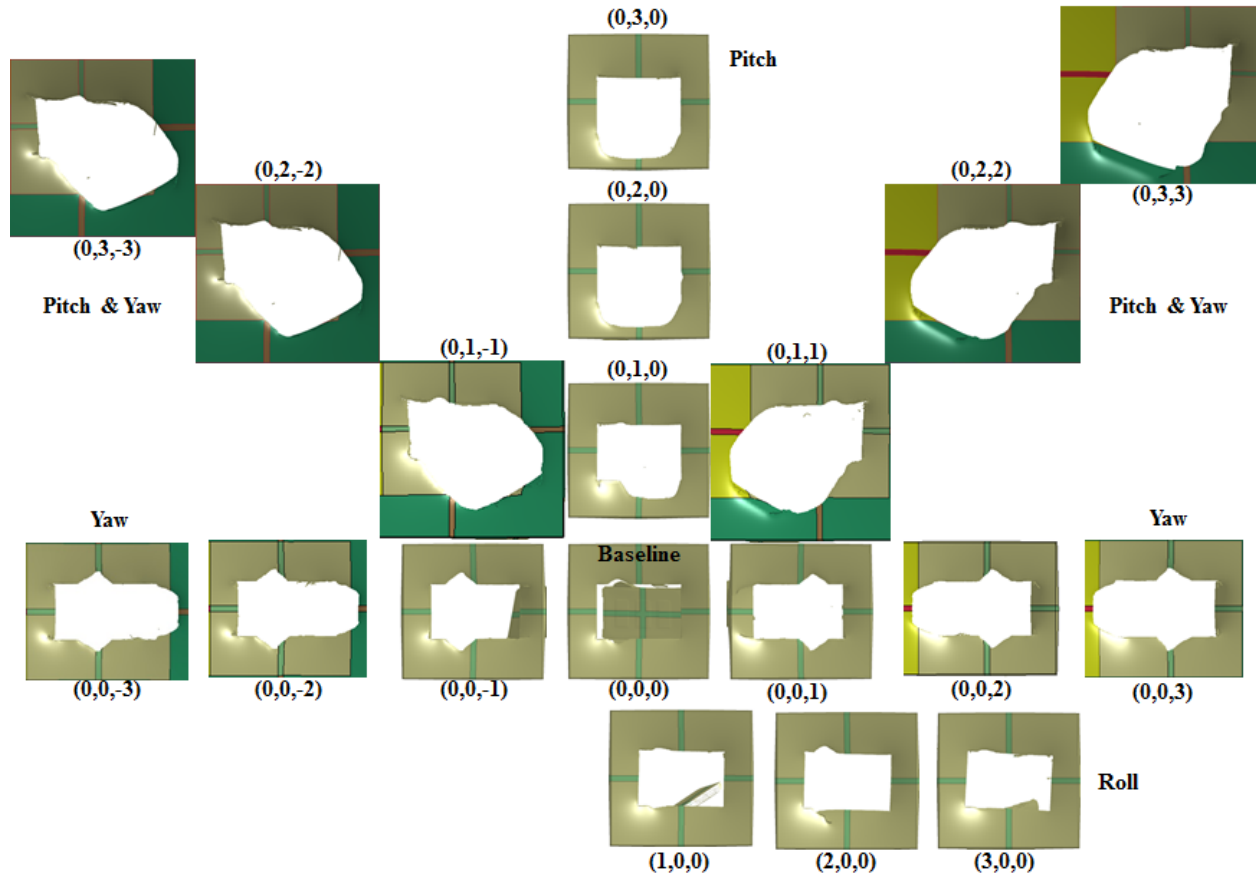


Figure 9. Penetration shapes in attitude angle variation series

Figure 10 shows the estimated range of ballistic limit velocity in attitude angle variation series. The ballistic limit velocities of the cases in attitude angle variation series was estimated by assuming that the exit velocity at the 400 fps impact velocity is the same regardless of the attitude angle variation, which is reasonable because the ballistic impact simulations showed that the exit velocity is not sensitive to the attitude angle at 400 fps impact velocity. The maximum and minimum fit curves were approximated by using the exit velocities points (orange small circles) in attitude angle variation series. The ballistic limit velocity of the baseline (#6.1.1) was estimated as 310 fps, and its variation range in the attitude angle variation series based on the baseline is estimated 16 fps from 307 fps (-3.5%) to 323 fps (1.6%), which is relatively small compared to the exit velocity variation range.

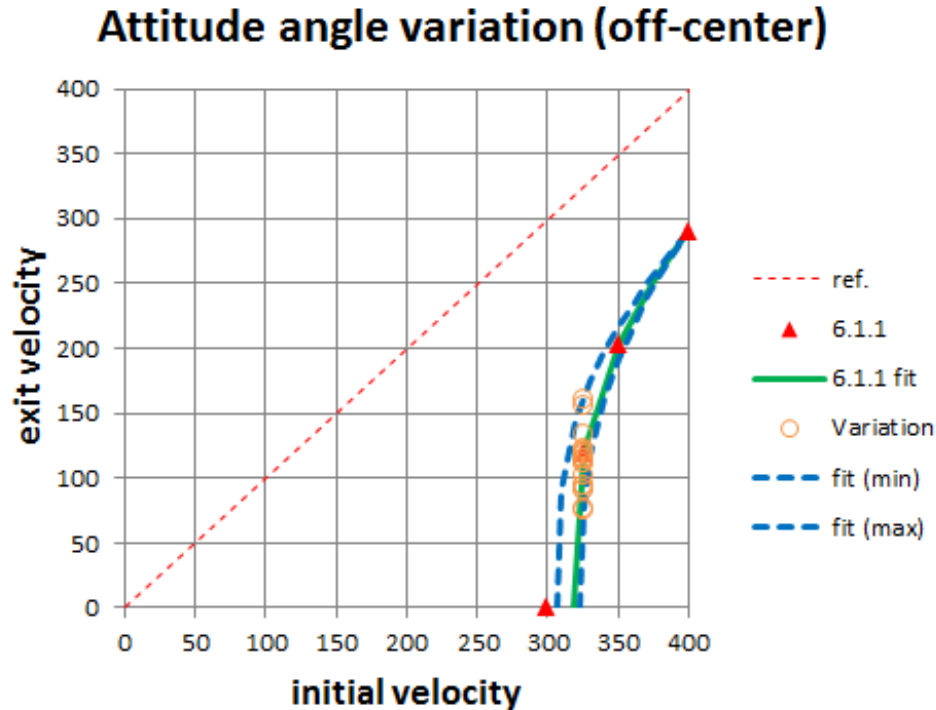


Figure 10. Estimated range of ballistic limit velocity in attitude angle variation series

Conclusion

In this research work, a series of ballistic impact simulations was conducted using LS-DYNA to simulate ballistic tests conducted at NASA that were run to provide data for validating *MAT_224 model (version 2.0) for Aluminum 2024. In the ballistic impact test setup, a rectangular parallelepiped shaped Inconel 718 projectile with sharp corners and edges impacts an Aluminum 2024 panel with various oblique and attitude angles, impact velocities, and impact points. *MAT_224 material models for Inconel 718 and Aluminum 2024 developed from specimen test data as part of this research program were used for the projectile and target plate. The simulations show good agreement with NASA ballistic impact experiments validating the Aluminum 2024 *MAT_224 model and illustrating the model predictive fidelity under challenging impact conditions.

Acknowledgements

The authors would like to express our gratitude to Dr. Mike Pereira, Aerospace Research Engineer at NASA Glenn Research Center, for sharing his insight and expertise along with the test photos and videos generated during the tests. His support greatly assisted with this research.

This research was conducted under FAA grant 13-G-020 and sponsored by the ACFPP.

References

- Børvik, T., Hopperstad, O. S. and Pedersen, K. O. (2010). "Quasi-brittle fracture during structural impact of AA7075-T651 aluminum plates," *International Journal of Impact Engineering*, Volume 37, Issue 5, Pages 537–551.
- Buyuk, M. (2014). "Development of a new metal material model in LS-DYNA part 2: Development of a tabulated thermo-viscoplastic material model with regularized failure for dynamic ductile failure prediction of structures under impact loading." Final Report, DOT/FAA/TC-13/25, P2.
- Dolci, S., Carney, K., Wang, L., Kan, C. D. and Du Bois, P. (2016). "Incorporation of inconel-718 material test data into material model input parameters for *MAT_224," 14th International LS-DYNA Users Conference, Dearborn MI.
- Emmerling, W., Altobelli, D., Carney, K. and Pereira, M. (2014). "Development of a new metal material model in LS-DYNA part 1: FAA, NASA, and industry collaboration background." Final Report, DOT/FAA/TC-13/25, P1.
- LSTC (2017). *LS_DYNA Keyword User's Manual*, Volume I and II, Version R10.0, Livermore, California.
- Park, C. K., Carney, K., Du Bois, P., Cordasco, D. and Kan, C. D. (2020). "Aluminum 2024-T351 input parameters for *MAT_224 in LS-DYNA," Final Report, DOT/FAA/TC-19/41 (In progress).
- Recht, R. F. and Ipson, T. W. (1963). "Ballistic perforation dynamics," *Journal of Applied Mechanics*, Volume 30, Pages 384–390.
- Ruggeri, C., Revilock, D., Pereira, M., Emmerling, W. and Queitzsch, G. (2015). "Impact and penetration of thin Aluminum 2024 flat panels at oblique angles of incidence." NASA/TM-2015-218484, DOT/FAA/TC-15/7.
- Seidt, J. D. (2014). "Development of a new metal material model in LS-DYNA part 3: Plastic deformation and ductile fracture of 2024 aluminum under various loading conditions." Final Report, DOT/FAA/TC-13/25, P3.